Contribution from the Department of Chemistry,
The University of North Carolina, Chapel Hill, North Carolina 27514

Intervalence Transfer in the Mixed-Valence Ion $[(bpy)_2(py)Ru(4,4'\text{-}bpy)Ru(py)(bpy)_2]^{5+}$

MICHAEL J. POWERS and THOMAS J. MEYER*

Received November 9, 1977

The mixed-valence ion $[(bpy)_2(py)Ru(4,4'\text{-}bpy)Ru(py)(bpy)_2]^{5+}$ (bpy is 2,2'-bipyridine, 4,4'-bpy is 4,4'-bipyridine, and py is pyridine), which is structurally similar to a $Ru(bpy)_3^{3+}$,$Ru(bpy)_3^{2+}$ contact ion pair, has been generated in solution by oxidation of the corresponding 4+ ion. The 4+ ion has been prepared and characterized as the PF_6^- salt. For the 5+ ion an absorption band appears in the near-infrared region which does not appear for either the 4+ or doubly oxidized 6+ ion. The near-IR band has been assigned to an intervalence transfer (IT) transition, but compared to closely related systems, the properties of the band are unusual. Although E_{op} (the energy of the near-IR absorption at λ_{max}) measured in a series of solvents does increase with $(1/n^2 - 1/D_s)$ (n^2 and D_s are the optical and static dielectric constants of the solvent medium), the relationship between the two may not be linear, and linearity is predicted by the Hush treatment for IT transitions. In addition, the sensitivity of E_{op} to changes in solvent as measured by the slope of a plot of E_{op} vs. $(1/n^2 - 1/D_s)$ is much less than theoretically predicted. The y intercept of the same plot is far higher than expected given recent results which estimate the rate of outer-sphere self-exchange between $Ru(bpy)_3^{2+}$ and $Ru(bpy)_3^{3+}$. The results obtained may indicate that thermal, intramolecular electron transfer is sufficiently rapid that solvent dielectric relaxation effects may become important. However, it is difficult to understand the relatively large values of E_{op} observed for the IT band.

Introduction

The results of recent experimental work using mixed-valence complexes of ruthenium[1-8] have been of value in pointing out the connection which was first suggested by Hush[9] between optical electron transfer in mixed-valence ions and thermal electron transfer in related systems. In an outer-sphere, self-exchange reaction such as

$$Ru(NH_3)_6^{3+} + Ru(NH_3)_6^{2+} \rightarrow Ru(NH_3)_6^{2+} + Ru(NH_3)_6^{3+} \quad (1)^{10}$$

or

$$(bpy)_2ClRu(py)^{2+} + (bpy)_2ClRu(py)^{+} \rightarrow (bpy)_2ClRu(py)^{+} + (bpy)_2ClRu(py)^{2+} \quad (2)^{11}$$

(bpy is 2,2'-bipyridine, py is pyridine), electron transfer occurs by initial ion-pair formation (eq 3) followed by electron transfer within the ion pair (eq 4). An activation barrier to

$$(bpy)_2ClRu(py)^{+} + (bpy)_2ClRu(py)^{2+} \rightleftharpoons (bpy)_2ClRu(py)^{+}, (bpy)_2ClRu(py)^{2+} \quad (3)$$

$$(bpy)_2ClRu^{II}(py)^{+}, (bpy)_2ClRu^{III}(py)^{2+} \rightarrow (bpy)_2ClRu^{III}(py)^{2+}, (bpy)_2ClRu^{II}(py)^{+} \quad (4)$$

electron transfer within the ion pair exists because both metal–ligand bond distances and the orientation of molecules in the outer coordination sphere respond to changes in the oxidation state at the metal. The same microscopic considerations also apply to optical (eq 5) and thermal (eq 6) electron transfer within dimeric or oligomeric[8,12,13] mixed-valence complexes in which there are localized redox sites on the vibrational time scale[4,6,8,9] (4,4'-bpy is 4,4'-bipyridine).

$$(bpy)_2ClRu^{II}(4,4'\text{-}bpy)Ru^{III}Cl(bpy)_2^{3+} \xrightarrow{h\nu} (bpy)_2ClRu^{III}(4,4'\text{-}bpy)Ru^{II}Cl(bpy)_2^{3+*} \quad (5)$$

$$(bpy)_2ClRu^{II}(4,4'\text{-}bpy)Ru^{III}Cl(bpy)_2^{3+} \xrightarrow{E_a} (bpy)_2ClRu^{III}(4,4'\text{-}bpy)Ru^{II}Cl(bpy)_2^{3+} \quad (6)$$

Application of the Franck–Condon principle to thermal electron transfer means that reorganization of the inner- and outer-coordination spheres must occur prior to electron transfer, and this is the basis for the classical barrier crossing treatments given by Hush[9] for intervalence transfer and by Marcus[15] and Hush[16] for outer-sphere electron transfer. More recent theoretical treatments have tended to emphasize the importance of electron–phonon coupling between the exchanging electron and the surrounding vibrational system and to point out that in thermal electron transfer, nuclear tunneling through the barrier may play an important role.[17,18]

In mixed-valence ions, the excess electron tends to be "trapped" at one site by differences in inner- and outer-coordination sphere vibrational modes. The differences exist because the oxidation states at the two metal sites are different. They are the origin of the intramolecular activation barrier to electron transfer in the mixed-valence ion.

Orbital overlap between the sites is promoted by mixing with ligand orbitals of the appropriate symmetry. With orbital overlap, electron delocalization occurs from Ru(II) to Ru(III). Delocalization mixes the oxidation state properties of the two sites and decreases the differences in the inner- and outer-coordination spheres. If overlap is sufficient, the barrier created by vibrational differences can be completely overcome and the two sites will be equivalent on the vibrational time scale which is a useful working definition for a delocalized system.

The extent of overlap needed for delocalization will clearly depend on the system involved. Increased orbital overlap leads to an increase in the electronic resonance energy which is needed to overcome the vibrational trapping energy. Reasonable estimates for the vibrational trapping energy in the absence of significant delocalization can be made. The estimates are based on outer-sphere, self-exchange measurements using complexes which have the chemical and physical properties of the redox sites in the mixed-valence ion; compare, for example, reactions 2 and 6.[2-4,6,14] If delocalization is extensive or the trapping energy (the activation barrier to electron transfer) is small, a transition from localized to delocalized states, or perhaps to some intermediate state between the two limiting descriptions, may be accessible. If the activation barrier is small, the delocalized state may be accessible even with slight orbital overlap.

Recently, a flash-photolysis technique was used to measure the rate of $Ru(bpy)_3^{3+}/Ru(bpy)_3^{2+}$ self-exchange.[19] The observed rate constant at 25 °C is near the diffusion-controlled limit and it has been concluded that the slight activation barrier arises largely from changes required in the outer-coordination sphere. This view is consistent with crystal structures of salts of the closely related ions $Fe(phen)_3^{2+}$[20] and $Fe(phen)_3^{3+}$[21] which show nearly identical Fe–N bond distances in the two ions.

We have prepared and isolated the ion $[(bpy)_2(py)Ru(4,4'\text{-}bpy)Ru(py)(bpy)_2]^{4+}$ and have generated the related 5+, mixed-valence ion in solution. The 5+ complex is essentially a $Ru(bpy)_3^{2+}$,$Ru(bpy)_3^{3+}$ dimer in which there is a chemical link between sites rather than the loose binding of a contact

0020-1669/78/1317-1785$01.00/0

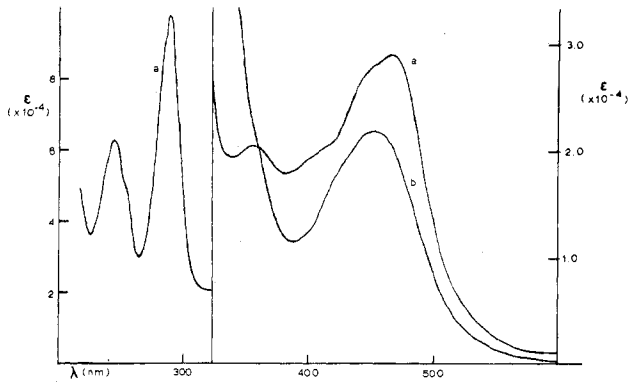

Figure 1. (a) UV–visible spectrum in CH_3CN of $[(bpy)_2(py)Ru(4,4'\text{-bpy})Ru(py)(bpy)_2]^{4+}$ and (b) visible spectrum of the 5+, mixed-valence dimer produced by one-electron oxidation using Ce(IV) as oxidant. The 5+ ion is reduced to the 4+ ion with time (see text).

ion pair although the Ru–Ru separation in the dimer (11.1 Å) is slightly shorter than the close contact distance (14.2 Å) within an ion pair.[22]

Our principal interest here was in the properties of the mixed-valence ion. The results of the outer-sphere, self-exchange experiment show that the vibrational trapping energy is small, and that suggests that the system might be delocalized or might be near the delocalized limit.

Experimental Section

Measurements. Ultraviolet, visible, and near-infrared spectra were recorded using Cary Model 14 and Model 17 and Bausch and Lomb UV210 spectrophotometers. Electrochemical measurements were made vs. the saturated sodium chloride calomel electrode (SSCE) at 25 ± 2 °C and are uncorrected for junction potentials. The measurements were made using a PAR Model 173 potentiostat for potential control and a PAR Model 175 universal programmer as a sweep generator for experiments. Elemental analyses were performed by Integral Microanalytical Labs, Raleigh, N.C.

Materials. Tetra-*n*-butylammonium hexafluorophosphate (TBAH) was prepared by standard techniques.[1b,25] Acetonitrile (MCB Spectrograde) was dried over Davidson 4-Å molecular sieves for electrochemical and spectral measurements. All solvents used were purchased commercially and purified according to standard procedures.[26,27]

Preparation of Complexes. $[(bpy)_2(py)Ru(4,4'\text{-bpy})Ru(py)(bpy)_2](PF_6)_4 \cdot 2H_2O$. $[Ru(bpy)_2(NO)py](PF_6)_3$[28] (0.608 g, 0.635 mmol) was dissolved in ~30 mL of acetone. KN_3 (0.052 g, 0.635 mmol) dissolved in a minimum (~5 mL) of methanol was added dropwise while protecting the stirred solution from light. After 15 min, a solution of 4,4'-bipyridine (0.061 g, 0.317 mmol) in acetone was added and the mixture heated at reflux under argon for 24 h. Toward the end of the reaction period, the acetone was distilled off and the mixture was taken to dryness. The bright orange complex was redissolved in a minimum of acetone, filtered through a medium glass frit into ~150 mL of stirred ether, and collected by suction filtration; yield ~95%. The complex was further purified by column chromatography on Al_2O_3 using $MeOH/CH_2Cl_2$ mixtures or CH_3CN/C_6H_6 mixtures for elution. The yield after chromatography was 70%. Anal. Calcd for $Ru_2C_{60}H_{52}N_{12}O_2P_4F_{24}$: C, 41.40; H, 2.99; N, 9.58. Found: C, 41.32; H, 2.76; N, 9.58.

$[(bpy)_2(py)Ru(4,4'\text{-bpy})Ru(py)(bpy)_2]^{5+,6+}$. The mixed-valence 5+ and Ru(III)–Ru(III) 6+ complexes were generated in solution by electrochemical means or by using $(NH_4)_2Ce(NO_3)_6$ as an oxidant. The complexes are remarkably effective oxidizing agents which prevented their isolation as pure solids. Solutions of the ions were generated as needed by oxidation of the 4+ ion in solution.

Results

Spectral and Redox Properties. The optical spectrum of $[(bpy)_2(py)Ru(4,4'\text{-bpy})Ru(py)(bpy)_2]^{4+}$ in acetonitrile is shown in Figure 1. It is very similar in detail to the spectrum of $Ru(bpy)_3^{2+}$[29] except for the appearance of a shoulder on the high-energy side of the 450-nm band. Given the similar assignments made in related complexes, the shoulder may well have its origin in a $(Ru^{II})d\pi \rightarrow \pi^*(4,4'\text{-bpy})$ transition which is strongly red-shifted in the dimer because of the remote $Ru(py)(bpy)_2$ group.[1,3,30] Because of the remarkable excited-state properties of $Ru(bpy)_3^{2+}$,[4a,31] an attempt was made to observe luminescence from the dimer in an alcohol glass at 77 K. A weak luminescence was observed at λ_{max}(uncor) 610 nm. The observed luminescence feature occurs at the same energy as λ_{max} for $Ru(bpy)_3^{2+}$[31] and related monomeric complexes and is sufficiently weak that it may originate from an impurity in the sample.

A cyclic voltammogram of the dimer in 0.1 M $[N(n\text{-}C_4H_9)_4](PF_6)$ vs. SSCE at 25 ± 2 °C includes only a single, broad oxidative wave and its corresponding reductive component (ΔE_p = 90 mV; $E_{1/2}$ = 1.36 V) at potentials more positive than 0 V. This behavior is typical of Ru–Ru dimers where the bridging ligand is 4,4'-bipyridine, *trans*-1,2-bis(4-pyridyl)ethylene, or 1,2-bis(4-pyridyl)ethane. For such complexes only a single broad wave is observed in the potential region of the Ru(III)/Ru(II) couples for related monomeric complexes. In fact, the cyclic voltammograms consist of two, closely spaced one-electron waves corresponding to the successive oxidations of the 4+ ion to the 5+ ion and of the 5+ ion to a 6+ ion.[3,4b,32] Coulometry at anodic potentials past the broad oxidation wave gave n values that were consistently >2 and rereduction gave $n < 2$. The problem with the coulometric results is that solutions of the 6+ ion are unstable. The 6+ ion slowly oxidizes the solvents used or trace water or other impurities in them. With time, reduction of the 6+ ion to the 5+ ion and more slowly of the 5+ ion to the 4+ ion can be observed spectrophotometrically in all of the solvent media used. The instability toward reduction of the 6+ ion has prevented us from isolating it as a pure, stable salt free of the 5+ ion. The same problem has been encountered in the attempted preparation of stable salts of $Ru(bpy)_3^{3+}$.[29,33]

Formal potentials for the 6+/5+ and 5+/4+ couples (eq 7 and 8) must be separated by at least 36 mV on the basis of

$$[(bpy)_2(py)Ru(4,4'\text{-bpy})Ru(py)(bpy)_2]^{6+} + e^- \rightarrow [(bpy)_2(py)Ru(4,4'\text{-bpy})Ru(py)(bpy)_2]^{5+} \quad (7)$$

$$[(bpy)_2(py)Ru(4,4'\text{-bpy})Ru(py)(bpy)_2]^{5+} + e^- \rightarrow [(bpy)_2(py)Ru(4,4'\text{-bpy})Ru(py)(bpy)_2]^{4+} \quad (8)$$

the existence of statistical factors for the two couples.[2,3,4b] As a result there is a statistical factor of 4 favoring the comproportionation equilibrium in eq 9 which means that for eq 9, $K \geq 4.0$.

$$[(bpy)_2(py)Ru(4,4'\text{-bpy})Ru(py)(bpy)_2]^{6+} + [(bpy)_2(py)Ru(4,4'\text{-bpy})Ru(py)(bpy)_2]^{4+} \rightleftharpoons 2[(bpy)_2(py)Ru(4,4'\text{-bpy})Ru(py)(bpy)_2]^{5+} \quad (9)$$

The 5+, mixed-valence ion was generated in solution by controlled-potential electrolysis of the 4+ ion at 1.6 V vs. the SSCE. Oxidation to n = 1 gave a solution containing an equilibrium mixture of the 4+, 5+, and 6+ ions (eq 9). The stability of such solutions was sufficient that spectral data could be obtained before appreciable net reduction of the 5+ ion to the 4+ ion had occurred. In Figure 1b is shown an optical spectrum obtained after oxidizing the 4+ ion in acetonitrile by 1 equiv of Ce(IV). A general decrease in absorbance is observed in the visible spectrum with no new absorption bands appearing.

Near-Infrared Spectral Properties. In the near-infrared spectral region, the 4+ and 6+ dimers are transparent, but an absorption band appears for the 5+, mixed-valence ion as shown in Figure 2. The mixed-valence ion was generated electrochemically in a series of solvents and the properties of the near-IR bands observed are summarized in Table I. Given also in Table I are values of $\Delta\bar{\nu}_{1/2}$[34] (the spectral bandwidth

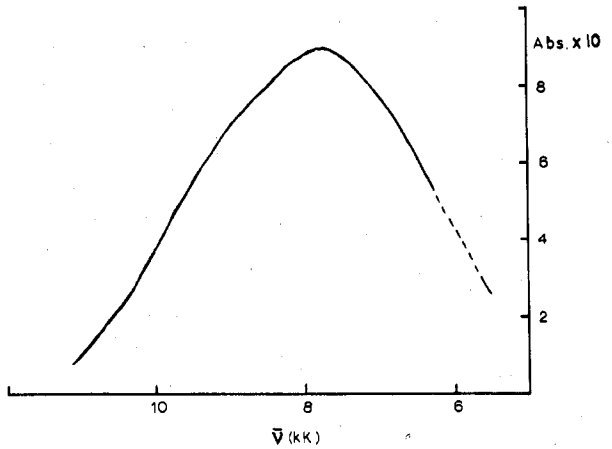

Figure 2. Near-infrared spectrum of $[(bpy)_2(py)Ru(4,4'\text{-}bpy)Ru(py)(bpy)_2]^{5+}$ in 0.1 M $[N(n\text{-}C_4H_9)_4](PF_6)/CH_3CN$. The mixed-valence ion was generated by electrolysis of the 4+ ion until $n = 1$.

Table I. Near-Infrared Spectral Data for $[(bpy)_2(py)Ru(4,4'\text{-}bpy)Ru(py)(bpy)_2]^{5+}$

Solvent[a]	$1/n^2 - 1/D_s$	E_{op}, $cm^{-1} \times 10^3$	$\Delta\bar{\nu}_{1/2}$ (obsd), $cm^{-1} \times 10^3$	$10^3 f$[b]	$10^4 \alpha^2$[b]
Acetonitrile	0.526	7.90 ± 0.1[c]	4.10	1.7–3.4	1.6–3.2
D_2O[d,e]	0.546	7.50 ± 0.05	4.05	2.3–4.6	2.3–4.6
Nitrobenzene	0.384	7.10 ± 0.05	3.90	2.6–5.2	2.7–5.4
Propylene carbonate	0.481	7.40 ± 0.05	4.94		
Nitromethane	0.498	7.55 ± 0.05	3.86		
Benzonitrile	0.388	7.30 ± 0.05	4.20		

[a] 0.1 M in $[N(n\text{-}C_4H_9)_4](PF_6)$. [b] The ranges reported for the values of f and α^2 were calculated assuming for the high number that oxidation of the 4+ ion gives the mixed-valence 5+ ion only. The low values were calculated assuming that $K = 4$ for the conproportionation equilibrium in eq 9. [c] Average of five experiments. [d] 0.1 M DCl/D_2O. [e] Mixed-valence ion generated using Ce(IV).

at half-height), the oscillator strengths f[34] where these values were obtainable, and values of α^2 calculated using equation 10.[9] In eq 10, ϵ_{max} is the maximum molar extinction coef-

$$\alpha^2 = \frac{(4.2 \times 10^{-4})\epsilon_{max}\Delta\bar{\nu}_{1/2}}{\bar{\nu}_{max}d^2} \qquad (10)$$

ficient for the near-IR band, $\bar{\nu}_{max}$ is the energy of the band, and d is the Ru–Ru separation. For mixed-valence ions where the valences are localized, α^2 gives an estimate of the extent of delocalization of the extra electron in the ground state.[9,35] Exact values for α^2 and f could not be calculated because equilibrium constants for the conproportionation equilibrium in eq 9 are not known. The data in Table I are given as a range in α^2 and f. The low values were calculated assuming $K = 4$ for eq 9 and the high values assuming that one-electron oxidation of the 4+ ion gives the mixed-valence ion only. The actual values are somewhere within the ranges reported.

Previous work on near-IR bands using mixed-valence Ru–bpy ions has been carried out in dilute solutions with no added electrolyte. Since the convenient generation of $[(bpy)_2(py)Ru(4,4'\text{-}bpy)Ru(py)(bpy)_2]^{5+}$ involved electrochemical oxidation, it was necessary to have an added supporting electrolyte. A test of the effect, if any, of added electrolyte on near-IR band properties was made by generating the 5+ ion in a series of solutions where the concentrations of added supporting electrolyte, $[N(n\text{-}C_4H_9)_4](PF_6)$, were varied over the range 0.01–0.2 M in acetonitrile. As found previously for the ion $[(NH_3)_5Ru(pyr)RuCl(bpy)_2]^{4+}$,[1b] there

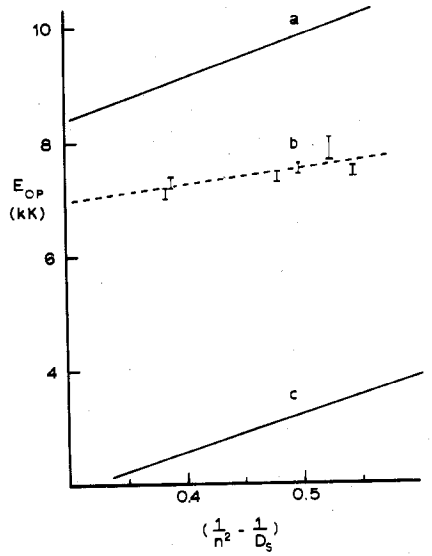

Figure 3. Plot of E_{op} vs. $(1/n^2 - 1/D_s)$ for $[(bpy)(py)Ru(4,4'\text{-}bpy)Ru(py)(bpy)_2]^{5+}$, b, and for $[(bpy)ClRu(4,4'\text{-}bpy)RuCl(bpy)_2]^{3+}$, a. Plot c is a calculated line assuming $\lambda_i = 0$ (see text).

was no systematic shift in $\bar{\nu}_{max}$ with added electrolyte and the observed values were all at $(7.9 \pm 0.1) \times 10^3$ cm^{-1} (1 kK ≡ 10^3 cm^{-1}).

In Figure 3 is shown a plot of E_{op} ($\bar{\nu}_{max}$, the energy of the near-IR transition) vs. $(1/n^2 - 1/D_s)$. n^2 and D_s are the optical and static dielectric constants for the pure solvents. The use of static dielectric constant values for the pure solvents would appear to be justified, at least for the cases where $[N(n\text{-}C_4H_9)_4](PF_6)$ is the added supporting electrolyte. For such large ions, dielectric saturation effects are expected to be small[36a] and at the dilute concentrations used, corrections for the volume fraction occupied by the electrolyte are negligible.[36b] For purposes of comparison, a similar plot is shown for the mixed-valence ion $[(bpy)_2ClRu(4,4'\text{-}bpy)RuCl(bpy)_2]^{3+}$.[14,37] The comparison between the two plots is instructive since the bridging ligand is the same in both ions and they differ only in the ligand occupying the sixth coordination site. From the plots for the two ions the following parameters were obtained: (1) for $[(bpy)_2ClRu(4,4'\text{-}bpy)RuCl(bpy)_2]^{3+}$, slope = 7.9×10^3 cm^{-1} Å^{-1}, y intercept = 6.0×10^3 cm^{-1}, correlation coefficient $r = 0.99$; (2) for $[(bpy)_2(py)Ru(4,4'\text{-}bpy)Ru(py)(bpy)_2]^{5+}$, slope = 3.1×10^3 cm^{-1} Å^{-1}, y intercept = 6.0×10^3 cm^{-1}, $r = 0.79$.

Discussion

Spectral and Redox Properties. The spectral and redox properties of the ion $[(bpy)_2(py)Ru(4,4'\text{-}bpy)Ru(py)(bpy)_2]^{5+}$ are consistent with the presence of discrete, weakly interacting Ru(II) and Ru(III) sites. The $E_{1/2}$ values (1.29 V in 0.1 M $[(n\text{-}C_4H_9)_4](PF_6)/CH_3CN$) and the absorption spectrum in the visible region are very nearly those for an equimolar mixture of $Ru(bpy)_3^{3+}$ and $Ru(bpy)_3^{2+}$ in CH_3CN.

Near-Infrared Spectral Properties. The properties of the near-IR band for the 5+ dimer are somewhat unusual both when compared to the theoretical predictions made by Hush and when compared to experimental results obtained for the ions $[(bpy)_2ClRu^{II}(L)Ru^{III}Cl(bpy)_2]^{3+}$. The most useful comparison is with the ion $[(bpy)_2ClRu^{II}(4,4'\text{-}bpy)Ru^{III}Cl(bpy)_2]^{3+}$ and plots of IT band energies vs. $(1/n^2 - 1/D_s)$ are shown for both complexes in Figure 3.

Hush has derived eq 11 for the variation of E_{op} with the

$$E_{op} = \lambda_i + (me)^2(a_1/2 + a_2/2 - 1/d)(1/n^2 - 1/D_s) \qquad (11)$$

dielectric properties of the surrounding medium.[9] In eq 11, m is the extent of charge transfer in the IT process, e is the

unit electron charge, a_1 and a_2 are the molecular radii at the electron donor and acceptor sites, d is the internuclear separation between sites, n^2 and D_s are the optical and static dielectric constants of the medium, and λ_i is the inner coordination sphere contribution to E_{op}.

E_{op} is the energy difference between the ground and vertical mixed-valence excited state (eq 5). If delocalization is slight, E_{op} is determined by the excess vibrational energy content of the excited state over the ground state. Optical excitation, which occurs instantaneously on the vibrational time scale, produces Ru(II) and Ru(III) sites in the equilibrium coordination environments of the other oxidation state.

In the derivation of eq 11, it is assumed that the contributions to E_{op} from inner coordination sphere vibrational modes (λ_i) are separable from contributions from the lower frequency modes of the surrounding solvent and that the solvent (outer sphere) contributions can be treated using a dielectric continuum model. Using this model and treating the redox sites as spheres give $\lambda_0 = (me^2)(a_1/2 + a_2/2 - 1/d)(1/n^2 - 1/D_s)$ which is the second term in eq 11.[9,38]

From eq 11, a plot of E_{op} vs. $(1/n^2 - 1/D_s)$ should be linear with slope $(me)^2(^1/_2a_1 + {}^1/_2a_2 - 1/d)$ and intercept λ_i.[39] From Figure 3, for the ion $[(bpy)_2ClRu^{II}(4,4'\text{-bpy})Ru^{III}Cl(bpy)_2]^{3+}$ in six solvents the expected linearity is found ($r = 0.99$), the intercept, $\lambda_i = 6.3 \times 10^3$ cm^{-1}, is the same within experimental error as values found for the ions $[(bpy)_2ClRu^{II}(BPE)Ru^{III}Cl(bpy)_2]^{3+}$ and $[(bpy)_2ClRu^{II}(pyr)Ru^{III}Cl(bpy)_2]^{3+}$,[2,14] and the observed (7.91×10^3 cm^{-1}/Å) and calculated (7.13×10^3 cm^{-1}/Å) slopes are in excellent agreement.

For the calculated values of the slope, the internuclear separation d (see eq 11) was taken to be 11.1 Å. On the basis of the known crystal structures of salts of $Fe(phen)_3^{2+}$ [20] and $Fe(phen)_3^{3+}$,[21] it was assumed that $a_1 = a_2$. a_1 was calculated to be 6.4 Å from the average value of the four Ru–bpy edge distances (7.1 Å), half the Ru–Ru separation (5.64 Å), and the Ru–Cl distance (4.2 Å).[40] The Ru–bpy edge distance was calculated from the crystal structure of $Fe(phen)_3^{2+}$ using the reported bond distances, 1.1 Å for the van der Waals radius of hydrogen[24] and correcting for the difference in Ru–N[23] and Fe–N bond distances.[20,21] The smaller values (5.7 Å) used earlier were based on metal–edge distances[41] which did not include the van der Waals radius for hydrogen.[2,3] Similar although less precise agreement between experiment and theory has also been found for two mixed-valence biferrocene ions.[42]

The situation is far less satisfying for the ion $[(bpy)_2(py)Ru(4,4'\text{-bpy})Ru(py)(bpy)_2]^{5+}$. If a straight line is drawn through the points in Figure 3, the y intercept is 6.0×10^3 cm^{-1}, but the correlation coefficient is far lower (0.79) than obtained for the other systems, and it is not obvious from the data that a linear relationship actually exists. In Figure 3c is shown a theoretical line, $E_{op} = (6.5 \times 10^3 \text{ cm}^{-1}/\text{Å})(1/n^2 - 1/D_s)$, calculated using the molecular distances cited above[43] and assuming that $\lambda_i = 0$. In comparing Figure 3b and c, it is clear that the experimental slope (3.1×10^3 cm^{-1}/Å) is far less than the calculated value of 6.5×10^3 cm^{-1}/Å showing that the IT band energy is much less responsive to changes in solvent dielectric properties than predicted. The intercept of the plot is essentially the same as that found for $[(bpy)_2ClRu(4,4'\text{-bpy})RuCl(bpy)_2]^{3+}$. The value seems to be unreasonably high given the structural data for the $Fe(phen)_3^{2+}$ and $Fe(phen)_3^{3+}$ salts and the rapid $Ru(bpy)_3^{3+/2+}$ self-exchange rate which suggest that λ_i should be small.[19] For the chloro dimer, the properties of the IT band have been shown to be consistent with the independently estimated rate of $[Ru(bpy)_2(py)Cl]^{2+/+}$ self-exchange,[2,3] and the relatively large λ_i value may be reconcilable in terms of significant changes in the Ru–Cl bond distances with oxidation state,[5] although this point is not clear in the absence of x-ray structural information.

The magnitude of the α^2 values calculated here for $[(bpy)_2(py)Ru(4,4'\text{-bpy})Ru(py)(bpy)_2]^{5+}$ is also somewhat surprising. The value in 0.1 M $[N(n\text{-}C_4H_9)_4](PF_6)/CH_3CN$ ($(1.6\text{–}3.2) \times 10^{-4}$) is in the same range as α^2 for $[(bpy)_2ClRu(4,4'\text{-bpy})RuCl(bpy)_2]^{3+}$ in acetonitrile ($(2.16\text{–}4.32) \times 10^{-4}$) although it might be expected to be considerably lower. From reduction potential measurements, the substitution of a pyridine group for a chloride ion in Ru–bpy complexes causes a steady increase in reduction potential—$(bpy)_2RuCl_2^{+/0}$, $E_{1/2} = 0.31$ V; $(bpy)_2Ru(py)Cl^{2+/+}$, $E_{1/2} = 0.79$ V; $(bpy)_2Ru(py)_2^{3+/2+}$, $E_{1/2} = 1.30$ V—and the increase in potential is followed linearly by an increase in ν_{max} for the lowest $\pi^*(bpy) \leftarrow d\pi$ charge-transfer (CT) transition.[44] The increase in reduction potential with the number of pyridine-type ligands is thought to arise largely because of stabilization of Ru(II) by increased $d\pi \rightarrow \pi^*$ back-bonding. Back-bonding stabilizes the $d\pi$ levels and decreases the radial extension of the $d\pi$ orbitals along the remaining coordination directions. If the orbital mechanism for Ru(II)–Ru(III) overlap is $d\pi(Ru^{II}) \rightarrow \pi^*(4,4'\text{-bpy})$ mixing, which effectively carries the Ru^{II} $d\pi$ wave function across the bridge to Ru(III), a decrease in α^2 would be expected for $[(bpy)_2(py)Ru(4,4'\text{-bpy})Ru(py)(bpy)_2]^{5+}$ compared to the chloro dimer because of increased back-bonding to the nonbridging ligands. That such effects can be significant is suggested by the fact that $[(bpy)_2ClRu(pyr)RuCl(bpy)_2]^{3+}$ is a localized valence case while in $[(NH_3)_5Ru(pyr)Ru(NH_3)_5]^{5+}$, where there are no ligands competing for $d\pi(Ru^{II})$ electron density, enhanced Ru(II)–Ru(III) overlap apparently leads to equivalent Ru sites although the evidence is somewhat equivocal.[4,6,8]

A possible origin for the apparently anomalous behavior of the IT band for the pyridine dimer could be that the additional electron in the ion $[(bpy)_2(py)Ru(4,4'\text{-bpy})Ru(py)(bpy)_2]^{5+}$ is delocalized between sites, at least on the infrared time scale. In a delocalized ion the assignment of the near-IR absorption band would be to an optical transition between delocalized electronic levels, and the energy restrictions imposed by the Hush treatment for IT transitions would no longer apply nor would the usual interpretation of α^2 as being a measure of the extent of ground-state delocalization.

A completely delocalized description for the ion seems unlikely. For the Creutz and Taube ion $[(NH_3)_5Ru(pyr)Ru(NH_3)_5]^{5+}$, the near-IR band is far narrower than predicted for an IT transition. Its energy varies only slightly with changes in the dielectric properties of the medium,[46] and its bandwidth and temperature dependence are consistent with an origin involving a transition between delocalized electronic levels.[45] In contrast, the near-IR band for $[(bpy)_2(py)Ru(4,4'\text{-bpy})Ru(py)(bpy)_2]^{5+}$ is broad and does respond significantly to changes in solvent although to a lesser degree than expected.

For the pyridine mixed-valence ion, the surrounding solvent structure could be partially relaxed. Frequency-dependent studies show that in the microwave region molecular rotations of solvent molecules begin to lag behind the oscillations of an applied electric field which gives rise to dielectric loss effects.[36,47–49] From dielectric loss measurements, relaxation times of $\sim 10^{11}$ s have been determined for water and a number of polar organic solvents at room temperature. The rate constant k for intramolecular electron transfer in the ion $[(bpy)_2ClRu^{II}(pyr)Ru^{III}Cl(bpy)_2]^{3+}$ has been estimated to be $\leq 3 \times 10^{10}$ s^{-1} at room temperature.[3] If the frequency of electron oscillation in the ion $[(bpy)_2(py)Ru(4,4'\text{-bpy})Ru(py)(bpy)_2]^{5+}$ were in this range but slightly faster, dielectric loss effects would begin to influence its properties noticeably. A lag would occur between solvent rotation and the oscillating

electric field created by the exchanging electron. The simple assumption of a dielectric continuum would no longer apply. The contribution of the solvent to valence trapping would be dependent on the electron oscillation rate which would lead to an electron–phonon coupling between the exchanging electron and reorientations in the outer-coordination sphere.

Even if the rate of electron oscillation is sufficiently rapid to cause nearly complete dielectric relaxation in the solvent surrounding the ion, valence trapping may still exist on the vibrational time scale (10^{-12}–10^{-13} s). The trapping could occur because of differences in the inner-coordination spheres arising from the change in oxidation state at the two sites. The extent of trapping will depend on the force constants and distance changes involved since they determine the difference in vibrational energy between the activated complex for electron transfer and the equilibrium vibrational states.

The magnitude of the E_{op} values for the ion $[(bpy)_2(py)Ru(4,4'\text{-}bpy)Ru(py)(bpy)_2]^{5+}$ are a troubling feature. The data suggest that there may be a rather large contribution to E_{op} from λ_i. This would be a surprising result, once again, because of the nearly identical Fe–N bond distances found in salts of $Fe(phen)_3^{2+}$[20] and $Fe(phen)_3^{3+}$[21] and the rapid self-exchange rate for the $Ru(bpy)_3^{3+/2+}$ couple.[19]

If dielectric loss effects are important in the outer-coordination sphere around the mixed-valence ion because of rapid intramolecular electron transfer, no simple relationship can be expected between E_{op} and $(1/n^2 - 1/D_s)$. The extent of dielectric loss could vary considerably from solvent to solvent because of differences in solvent relaxation times. Differences in the deviations between the appropriate dielectric constant in the oscillating field of the exchanging electron and the static dielectric constant, D_s, could cause at least part of the scatter in the values shown in Figure 3. There would no longer be a basis for comparing the experimental data with a calculated slope based on the static dielectric constant of the solvent.

We are left with a dilemma because of the magnitude of E_{op} for the IT band. With complete or partial dielectric relaxation, the trapping energy exerted by the solvent arising from differences in solvation at the different oxidation state sites must decrease. This would decrease the energy difference between ground and mixed-valence excited states and thus E_{op}. The expected decrease could be compensated for in part by increased electron delocalization induced by electron–phonon coupling which would cause a greater splitting between surfaces. The system could still be localized on the infrared time scale because of incomplete dielectric relaxation and because of trapping by vibrational modes which occur at frequencies higher than the electron oscillation frequency.

Since molecular differences between oxidation state sites are probably slight, thermal electron transfer by nuclear tunneling through the barrier may be important and there may be no direct relationship between optical and thermal electron transfer. Such a model might explain the large bandwidths observed but not the values for E_{op}. A last factor which could affect E_{op} is an increased splitting between the mixed-valence excited-state and ground-state surfaces because of extensive orbital overlap between Ru(II) and Ru(III). Assuming that the near-IR band is an IT transition, the rather small value of α^2 argues against extensive delocalization in the ground state. In fact, it is hard to justify the existence of a significant electronic orbital overlap in the dimer given the localized nature of the valences in mixed-valence ions like $[(bpy)_2ClRu(4,4'\text{-}bpy)RuCl(bpy)_2]^{3+}$.

Acknowledgment. Acknowledgments are made to the Army Research Office, Durham, N.C., under Grant No. DAAG29-76-G-0135 for support of this research.

Registry No. $[(bpy)_2(py)Ru(4,4'\text{-}bpy)Ru(py)(bpy)_2](PF_6)_4$, 66240-33-3; $[(bpy)_2(py)Ru(4,4'\text{-}bpy)Ru(py)(bpy)_2]^{4+}$, 66240-32-2; $[(bpy)_2(py)Ru(4,4'\text{-}bpy)Ru(py)(bpy)_2]^{5+}$, 66455-86-5; $[(bpy)_2(py)Ru(4,4'\text{-}bpy)Ru(py)(bpy)_2]^{6+}$, 66269-56-5; $[Ru(bpy)_2(NO)py](PF_6)_3$, 29241-00-7.

References and Notes

(1) (a) R. W. Callahan, G. M. Brown, and T. J. Meyer, *J. Am. Chem. Soc.*, **96**, 7829 (1974); (b) *Inorg. Chem.*, **14**, 1443 (1975); (c) R. W. Callahan and T. J. Meyer, *Chem. Phys. Lett.*, **39**, 82 (1976).
(2) M. J. Powers, D. J. Salmon, R. W. Callahan, and T. J. Meyer, *J. Am. Chem. Soc.*, **98**, 6731 (1976).
(3) R. W. Callahan, F. R. Keene, T. J. Meyer, and D. J. Salmon, *J. Am. Chem. Soc.*, **99**, 1064 (1977).
(4) (a) T. J. Meyer, *Acc. Chem. Res.*, **11**, 94 (1978); (b) *Adv. Chem. Ser.*, **No. 150**, Chapter 7 (1976).
(5) M. J. Powers and T. J. Meyer, in preparation.
(6) T. J. Meyer, *Ann. N.Y. Acad. Sci.*, in press.
(7) G. Tom, C. Creutz, and H. Taube, *J. Am. Chem. Soc.*, **96**, 7827 (1974).
(8) H. Taube, *Ann. N.Y. Acad. Sci.*, in press.
(9) (a) N. S. Hush, *Prog. Inorg. Chem.*, **8**, 391 (1967); (b) *Electrochim. Acta*, **13**, 1005 (1968).
(10) Estimated by measuring the rate of the net reaction $Ru(ND_3)_6^{3+} + Ru(NH_3)_6^{2+} \rightarrow Ru(ND_3)^{2+} + Ru(NH_3)_6^{3+}$ (T. J. Meyer and H. Taube, *Inorg Chem.*, **7**, 2369 (1968)).
(11) Estimated by measuring the rate of the net reaction $(phen)_2ClRu(py)^{2+} + (bpy)_2ClRu(py)^+ \rightarrow (phen)_2ClRu(py)^+ + (bpy)_2ClRu(py)^{2+}$ (phen is 1,10-phenanthroline, bpy is 2,2'-bipyridine, and py is pyridine) for which $K = 1.0$.[3]
(12) G. M. Brown, D. O. Cowan, C. LeVanda, F. Kaufman, P. V. Roling, M. P. Rausch, and T. J. Meyer, *Inorg. Chem.*, **14**, 506 (1975).
(13) M. J. Powers, R. W. Callahan, D. J. Salmon, and T. J. Meyer, *Inorg. Chem.*, **15**, 894 (1976).
(14) R. W. Callahan, M. J. Powers, D. J. Salmon, and T. J. Meyer, in preparation.
(15) (a) R. A. Marcus, *J. Chem. Phys.*, **24**, 966 (1956); (b) *ibid.*, **43**, 679 (1965); (c) *Annu. Rev. Phys. Chem.*, **15**, 155 (1964).
(16) N. S. Hush, *Trans. Faraday Soc.*, **57**, 557 (1961).
(17) N. S. Hush, *Chem. Phys.*, **10**, 361 (1975).
(18) N. R. Kestner, J. Logan, and J. Jortner, *J. Phys. Chem.*, **78**, 2148 (1974); W. Smickler, *Ber. Bunsenges. Phys. Chem.*, **77**, 991 (1973); S. G. Christov, *ibid.*, **79**, 357 (1975); P. P. Schmidt, *J. Chem. Phys.*, **56**, 2775 (1972); V. G. Levich, *Adv. Electrochem. Eng.*, **4**, 249 (1966); R. R. Dogonadze in "Reactions of Molecules at Electrodes", N. S. Hush, Ed., Plenum Press, London, 1971.
(19) The measurements were actually made for the reaction $Ru(bpy)_3^{2+} + Ru(phen)_3^{3+} \rightarrow Ru(bpy)_3^{3+} + Ru(phen)_3^{2+}$ for which $\Delta G = 0$ (R. C. Young, F. R. Keene, and T. J. Meyer, *J. Am. Chem. Soc.*, **99**, 2468 (1977)).
(20) A. Zalkin, D. H. Templeton, and T. Ueki, *Inorg. Chem.*, **12**, 1641 (1973).
(21) J. Baker, L. M. Engelhardt, B. N. Figgis, and A. H. White, *J. Chem. Soc., Dalton Trans.*, 530 (1975).
(22) The Ru–Ru separation in the dimer was calculated using an average Ru–N bond distance of 2.12 Å[23] and standard C–H and C–N bond distances. The radii of the $Ru(bpy)_3^{2+/3+}$ ions were calculated using the same approach and known values from the structurally similar $Fe(phen)_3^{2+/3+}$ complexes.[20,21] Added to these radii was the van der Waals radius of hydrogen (1.1 Å[24]).
(23) H. C. Stynes and J. A. Ibers, *Inorg. Chem.*, **10**, 2304 (1971).
(24) L. Pauling, "The Nature of the Chemical Bond", Cornell University Press, Ithaca, N.Y., 1960.
(25) W. Lange and E. Müller, *Chem. Ber.*, **63**, 1058 (1930).
(26) P. T. Sawyer and J. L. Roberts, Jr., "Experimental Electrochemistry for Chemists", Wiley, New York, N.Y., 1974, pp 203–210.
(27) A. Weissberger, Ed., "Techniques of Organic Chemistry", Vol. VII, Interscience, New York, N.Y., 1955.
(28) J. B. Godwin and T. J. Meyer, *Inorg. Chem.*, **10**, 471 (1971).
(29) J. N. Braddock and T. J. Meyer, *J. Am. Chem. Soc.*, **95**, 3158 (1973).
(30) R. W. Callahan, Ph. D. Dissertation, The University of North Carolina, Chapel Hill, N.C., 1975.
(31) (a) J. P. Paris and W. W. Brandt, *J. Am. Chem. Soc.*, **81**, 5001 (1959); (b) J. N. Demas and G. A. Crosby, *ibid*, **93**, 2841 (1971); *J. Mol. Spectrosc.*, **36**, 72 (1968); (c) F. E. Lytle and D. M. Hercules, *J. Am. Chem. Soc.*, **91**, 253 (1969); (d) K. W. Hipps and G. A. Crosby, *ibid.*, **97**, 7042 (1975); (e) J. Van Houten and R. J. Watts, *ibid.*, **98**, 4853 (1976).
(32) G. M. Brown, Ph.D. Dissertation, The University of North Carolina, Chapel Hill, N.C., 1974.
(33) R. E. Simone and R. S. Drago, *J. Am. Chem. Soc.*, **92**, 2343 (1970).
(34) In the low-energy region, the near-IR bands tail into strong solvent background absorption bands which arise from overtone transitions. As a consequence, bandwidths at half-height could not always be determined for the low-energy side of $\bar{\nu}_{max}$ and the procedure suggested by Hush for calculating $\Delta\bar{\nu}_{1/2}$[9] was used only for the data in CH_3CN and D_2O. In the other solvents, the bandwidth at half-height was estimated by determining the bandwidth at half-height on the high-energy side of the band and doubling it. Values of the oscillator strength f were obtained using the formula given by Hush, $f = (4.6 \times 10^{-9})\epsilon_{max}\Delta\bar{\nu}_{1/2}$, in which ϵ_{max} is the extinction coefficient at the band maximum and $\Delta\bar{\nu}_{1/2}$ is the band half-width in cm^{-1}.[9]

(35) B. Mayoh and P. Day, *Inorg. Chem.*, **13**, 2273 (1974); *J. Am. Chem. Soc.*, **94**, 2885 (1972).
(36) (a) J. B. Hasted, *Dielectr. Relat. Mol. Processes*, **1**, Chapter 5 (1972); (b) R. Pottel and U. Kaatze, *Ber. Bunsenges. Phys. Chem.*, **73**, 437 (1968).
(37) M. J. Powers, Ph.D. Dissertation, The University of North Carolina, Chapel Hill, N.C., 1977.
(38) Cannon has derived a different expression for λ_o by treating ligand-bridged mixed-valence ions as prolate ellipsoids having the major cylindrical axis along the line joining the metal centers (R. D. Cannon, *Chem. Phys. Lett.*, **49**, 299 (1977)).
(39) E_{op} at the intercept corresponds experimentally to a measurement in a nonpolar solvent like CCl_4 where $n^2 \approx D_s$.
(40) L. H. Vogt, J. L. Katz, and S. E. Wiberly, *Inorg. Chem.*, **4**, 1152 (1965).
(41) J. C. Solenberger, Ph.D. Dissertation, Washington University, St. Louis, Mo., 1970.
(42) M. J. Powers and T. J. Meyer, *J. Am. Chem. Soc.*, in press.
(43) Calculated as described above, except using $a_1 = [5(7.1)\ \text{Å} + 5.6\ \text{Å}]/6 = 6.9\ \text{Å}$
(44) D. J. Salmon, Ph.D. Dissertation, The University of North Carolina, Chapel Hill, N.C., 1976.
(45) J. K. Beattie, N. S. Hush, and P. R. Taylor, *Inorg. Chem.*, **15**, 992 (1976).
(46) C. Creutz and H. Taube, *J. Am. Chem. Soc.*, **95**, 1086 (1973).
(47) M. Davies, *Q. Rev., Chem. Soc.*, **8**, 250 (1954).
(48) W. C. Price, *Annu. Rev. Phys. Chem.*, **11**, 133 (1960).
(49) C. P. Smythe, "Dielectric Behavior and Structure", McGraw-Hill, New York, N.Y., 1955.

Contribution from the Department of Chemistry, Stanford University, Stanford, California 94305

μ-Pyrazine Polynuclear Mixed-Valence Species Based on Trans Ruthenium Tetraammines

A. VON KAMEKE, G. M. TOM, and H. TAUBE*

Received June 6, 1977

Polynuclear μ-pyrazine complexes based on *trans*-tetraammineruthenium as the linking metal unit have been prepared in two series. In one, ammonia occupies the terminal trans position and in this series the number of ruthenium atoms, n, ranges from 3 to 6. In the other series, with n = 2, 3, and 4, the terminal trans ligand is pyrazine. For the ammonia capped series, cyclic voltammetry indicates that the terminal ruthenium atoms are oxidized first. In this series, only when n = 3 does the near-IR absorption give evidence of end-to-end electron transfer in the one-electron oxidation product of the fully reduced species. For this system, the fact that the conproportionation constant of 70 much exceeds the statistical value also points to the conclusion that there is end-to-end communication. The mixed-valence species derived from both series show absorption in the near-infrared, usually complicated by the possibility of more than one metal-to-metal charge-transfer process. As the chain length increases, the absorption for the fully reduced state corresponding to the $\pi^* \leftarrow \pi$d transition moves progressively to lower energy, reaching 726 nm for the species with n = 6. On oxidation, this absorption moves to higher energies and at the same time it decreases in intensity, finally disappearing in the fully oxidized state.

Introduction

In the study of mixed-valence molecules, it is of interest to bridge the gap between our understanding of electron transfer in simple chemical reactions and electron transfer as it is encountered in extended arrays of atoms such as semiconductors and conductors. There is hope of achieving this by the study of polynuclear mixed-valence molecules. Results for several such systems have already been described: with pyrazine (pz) as bridging group and $Ru(bpy)_2$ as the metal core,[1,2] the mixed-valence species derived from $[[(NH_3)_5Ru(L)]_2Ru(bpy)_2]^{6+}$ by oxidation,[3] and polyferrocene species.[4] The systems we describe are most closely related to those reported on in the first three references and the Creutz ion itself.[5] In our systems, pyrazine is the bridging group and each ruthenium bears at most two π-acid ligands. Other work[6] has shown that the properties of the Creutz ion are dramatically altered when most of the saturated ligands are replaced by unsaturated ones.

Our investigations have included species with as many as six ruthenium atoms linked by pyrazine. Covering as they have a large number of species, they are incomplete in important respects, but we believe that the descriptions of the preparations and of general properties warrant publication at this stage.

Experimental Section

Preparations. It is to be noted at the outset that efforts to link large units proved futile, and the strategy we followed in the first series involved the stepwise reactions of the neutral species *trans*-$[SO_3(NH_3)_4Ru(OH_2)]$ to form trans pyrazine capped species $[Hpz(Ru(NH_3)_4pz)_nH]^{2n+2}$ where n ranges from 1 to 4. Sulfite labilizes the trans position, so that substitution takes place readily (it must be remembered, however, that this labilization is accompanied by a much reduced affinity).[7] On acidifying a solution containing a ruthenium sulfito complex and oxidizing with H_2O_2, SO_3^{2-} is converted to SO_4^{2-}. When the resulting species is reduced, SO_4^{2-} is replaced by water, and this ligand in turn is replaced by pyrazine. The source of the sulfito complex is $[SO_2Ru(NH_3)_4Cl]Cl$.[8] The species $[(NH_3)_5Ru(pz)(Ru(NH_3)_4pz)_mRu(NH_3)_5]^{2n+4}$ with m = 1–4 were then prepared by the reaction of $(NH_3)_5RuOH_2^{2+}$ with the appropriate pyrazine capped complex. The methods of preparation ensure that all the species we have studied are trans. Argon was used for deaeration in all the procedures which are described.

[*trans*-$Ru(NH_3)_4(pzH)_2]Cl_4$. Three hundred milligrams of *trans*-$[Ru(NH_3)_4(SO_2)Cl]Cl$ and an equal weight of pyrazine (pz) were dissolved in 4 mL of deaerated water, and the pH was adjusted to 7–8 using $NaHCO_3$. The solution was left for 5–10 min in the dark, acidified to about 1 M with HCl (no significant color change), and when CO_2 evolution had almost ceased, 30% H_2O_2 was added with stirring, until the color changed to a greenish brown. The mixture was added to a stirred solution of a 20-fold larger volume of concentrated HCl/acetone (1:19 by volume). Stirring was continued for several minutes and the solution was then cooled in the refrigerator for 1–2 h. The precipitate was collected, washed with acetone followed by ether, and dried in vacuo (yield >60%). The dried product has $[Ru(NH_3)(SO_4)pz]Cl$ as the major component. A total of 100 mg of the latter was dissolved in 2 mL of 0.01 M HCl and the solution was deaerated and reduced with zinc amalgam. Pyrazine (350 mg) was added, and after 2 h in the dark, the solution was poured into 2 mL of concentrated HCl + 40 mL of acetone while stirring. On storing in the refrigerator for 2 h, the precipitate was collected, washed with ether and acetone, and dried under vacuum (yield about 50%, without purification by gel filtration).

$[HpzRu_2pzH]Cl_6$. The first part of the preparation follows that just described except that 100 mg of $[Ru(NH_3)_4SO_2Cl]Cl$ and 12 mg of pyrazine were dissolved in 3 mL of deaerated water (after addition of $NaHCO_3$ the solution was dark red). The solid product of the oxidation by H_2O_2 (in this case the solution is yellowish green brown after a sufficient quantity of H_2O_2 is added) is $[SO_4Ru_2SO_4]Cl_2$

0020-1669/78/1317-1790$01.00/0